Simultaneous acquisition of two 2D HSQC spectra with different ^{13}C spectral widths

Pau Nolis, Kumar Motiram-Corral, Míriam Pérez-Trujillo, Teodor Parella *

Servei de Ressonància Magnètica Nuclear, Universitat Autònoma de Barcelona, E-08193, Bellaterra, Barcelona, Catalonia, Spain

ARTICLE INFO

ABSTRACT

A time-efficient NMR strategy that involves the interleaved acquisition of two 2D HSQC spectra having different spectral widths in the indirect ^{13}C dimension is presented. We show how the two equivalent coherence transfer pathways involved in sensitivity-enhanced HSQC experiments are managed selectively and detected separately in different FID periods within the same scan. The feasibility of this new SADA-HSQC (*Spectral Aliasing in Dually Acquired HSQC*) technique is demonstrated by recording simultaneously two complementary datasets, conventional and highly-resolved spectral-aliased 2D HSQC spectra, in a single NMR experiment. Combining the information from both datasets, accurate chemical shift determination and excellent signal dispersion is achieved in a unique measurement using only few t_1 increments.

© 2019 Elsevier Inc. All rights reserved.

1. Introduction

The digital resolution that is achieved along the indirect ^{13}C dimension (DR1) in 2D HSQC spectra is directly proportional to the number of collected t_1 increments (TD1) and indirectly proportional to the ^{13}C spectral width (SW1) to be monitored. Several techniques are available to improve such DR1, for instance, incorporating ^{13}C band-selective excitation into the pulse scheme and reducing SW1 to the region of interest [1,2], using non-uniform sampling (NUS) to reduce the effective TD1 [3–5], or applying resolution-enhanced data processing tools such as zero-filling or linear prediction [6]. Another simple but powerful approach to increase DR1 without changing the original pulse program or the acquisition mode is the re-acquisition of a second HSQC dataset with a reduced SW1. Thus, the DR1 before processing is 377.3 Hz/pt for a 2D HSQC experiment acquired with 128 t_1 increments and SW1 = 160 ppm at 600 MHz. On the other hand, by merely setting SW1 to a small value of 5 ppm, DR1 is improved by a factor of 32 until 11.8 Hz/pt without practically changing the duration of the experiment. The inconvenient of such an approach is that cross-peaks appear folded or aliased depending on the quadrature detection method applied in the indirect dimension. Sometimes, the concepts of spectral aliasing (SA) and spectral folding have been used indistinctly, introducing some confusion.

To clarify, Echo-anti/echo, States or States-TPPI quadrature detection in F1 affords aliased (superimposed) signals whereas TPPI generates folded (mirrored) signals [9]. For instance, a ^{13}C signal resonating at 110 ppm appeared at 10 ppm in an aliased HSQC experiment using an SW1 of 100 ppm and centered to 50 ppm. On the other hand, this same signal would appear at 90 ppm in the equivalent folded HSQC spectrum. Specifically, the regular sensitivity-enhanced HSQC (SE-HSQC) scheme uses the echo-anti/echo protocol to obtain pure absorption lineshapes [7,8], and signals are aliased in the resulting spectral-aliased HSQC (SA-HSQC) spectrum. The superimposed character of aliased signal allows a simple and accurate determination of true chemical shifts ($\delta(^{13}C)^{true}$) by applying Eq. (1):

$$\delta(^{13}C)^{true} = \delta(^{13}C)^{aliased} \pm \kappa * SW1^{aliased} \qquad (1)$$

where κ is the aliasing factor which depends on the ^{13}C frequency carrier and SW1^{aliased} is the spectral width utilized in the aliased experiment [9–12]. SA has been reported for several 2D experiments and some computer-aided spectral reconstruction procedures have been proposed to recover the classical spectral representation with their full spectral width [13–16]. In contrast to other experiments, SA is particularly recommended in HSQC because each ^{1}H signal only correlates with its directly attached ^{13}C nucleus, minimizing misassignments and allowing direct analysis and an accurate determination of $\delta(^{13}C)$ values without the need of specialized reconstruction programs. [17] Several options have been proposed to determine the signal-dependent κ factor: from

---

* Corresponding author.
  E-mail address: teodor.parella@uab.cat (T. Parella).

a regular 1D ^{13}C{^{1}H} or DEPT spectrum, [18] using a reference 2D HSQC spectrum with its full SW1, or acquiring two aliased datasets with slightly different SW1 [10,14,15,19]. All these options are time-consuming because two different datasets need to be recorded separately. We have also demonstrated that superb resolution conditions are achieved when SA in the F1 dimension and real-time broadband homodecoupling in the F2 dimension are simultaneously incorporated in the SAPS-HSQC (*Spectral Aliased Pure Shift* HSQC) experiment. The power of the SAPS-HSQC method to afford ultra-high-resolution 2D NMR maps has been demonstrated in enantiodifferentiation NMR studies [20], to discern between diastereoisomers with near-identical ^{1}H and ^{13}C NMR spectra [21] and to measure the sign and the magnitude of small coupling constants with high accuracy. [22] Definitively, the SA method is a clear competitor, and also compatible, to other F1 resolution-enhanced methods such as pure shift NMR, NUS or linear prediction.

We present here a novel time-efficient strategy for the simultaneous acquisition of both the reference and the aliased HSQC spectra using a single pulse scheme. Our proposal is based on the implementation of multiple-FID acquisition within the same scan (MFA) [23]. For instance, MFA offers the possibility to acquire simultaneously 2D COSY and 2D TOCSY experiments or 2D HMBC and 2D HMBC-TOCSY experiments using a single acquisition in spectrometers having a basic single-receiver configuration. This approach recovers the afterglow magnetization that remains active in the transverse plane after conventional FID acquisition. MFA has also been combined with other time-efficient NMR strategies such as time-sharing NMR. As an example, the recording of multiple FIDs in time-shared ^{1}H-^{13}C, ^{1}H-^{15}N HMBC affords four different HMBC spectra in a single collection step [24]. The proposal outlined here uses a different MFA approach based on the management of the two active coherence transfer pathways (CTP) involved in SE-HSQC and their separate detection in two different FID periods [25]. In contrast to the afterglow MFA method, the success of this approach relies on the fact that one of the components resides in the z-axis whereas the other one is detected. After this first detection period (FID1), a purge gradient is applied to remove any residual transverse magnetization and the second component becomes observable in a second acquisition (FID2) by a final 90° pulse.

2. Results and discussion

The proposed SADA-HSQC (*Spectral Aliasing in Dually Acquired HSQC*) experiment is displayed in Fig. 1. The SADA-HSQC pulse scheme handles the two components detected jointly in the SE-HSQC experiment in a separate way, allowing them a different behaviour during a double-stage variable evolution period and detecting them separately in different FID periods into the same pulse sequence. The method is related to the DENA (Differential Evolution for Non-ambiguous Aliasing) [14,19] and AMNA (Additional Modulation for Non-ambiguous Aliasing) [19] HSQC experiments where two different aliased signals were simultaneously detected taking advantage of a differential evolution of carbon chemical shift that encodes the aliasing factor. The analysis of these experiments needs a separate HSQC spectrum as a reference, and the aliased spectrum contains two different components than double the number of cross-peaks and therefore increases the probability of signal overlap.

To analyse how SADA-HSQC works, we start with the two operators available at the end of the first t_1 period, I_zS_x (term I) and I_zS_y (term II). After this period, a 90° (^{13}C) pulse retains the first term unaltered in the transverse plane while the term II is converted to zz magnetization. A second λ-scaled t_1 evolution time is applied to allow further ^{13}C chemical shift evolution exclusively for term I. Thus, term I evolves during $λ * t_1$ with a dephasing gradient effect proportional to G2 + G2 whereas term II evolves exclusively during t_1 with a dephasing proportional to G2. After this second variable period, a 90° (^{1}H) pulse converts term I to multiple-quantum coherences (I_yS_x) whereas the term II is converted to anti-phase (AP) ^{1}H magnetization (I_xS_z) which evolve to in-phase (IP) magnetization (I_y) in the subsequent echo period. The following 90° pulses applied to both ^{1}H and ^{13}C from the y-axis, convert term I in AP ^{1}H magnetization (I_yS_z) whereas term II is stored as I_z magnetization. The subsequent echo period refocuses term I to IP magnetization which is detected during the FID1 period whereas term II remains unused along the z-axis. After that, a purging gradient is
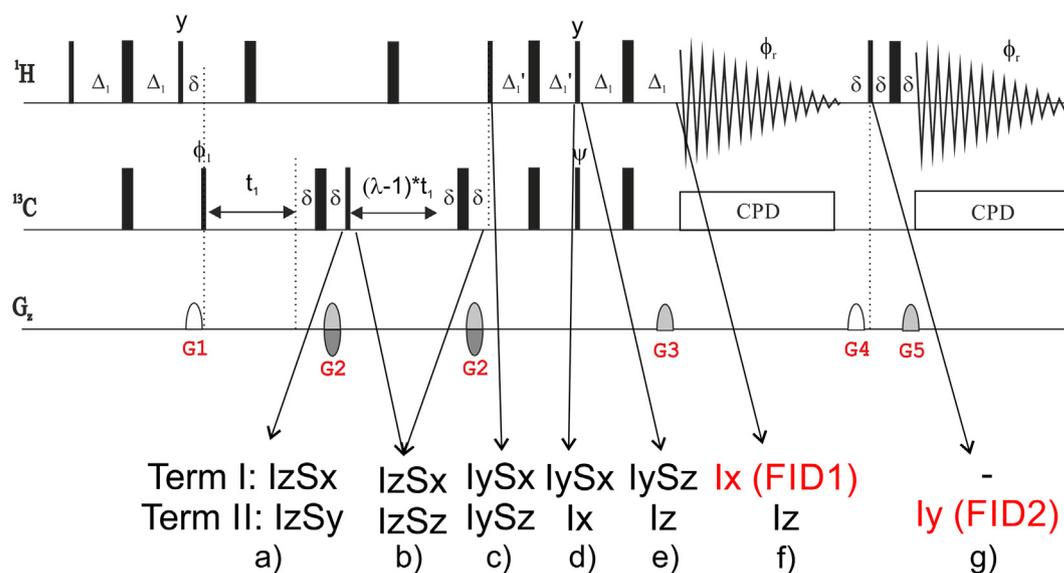

Fig. 1. Pulse sequence scheme of the SADA-HSQC experiment designed to record two HSQC datasets with different ^{13}C spectral windows in an interleaved mode. The two active terms in each key point into the sequence are shown. Narrow and wide filled bars correspond to 90° and 180° pulses, respectively, with phase x unless indicated otherwise. The inter-pulse delays were optimized to $Δ_1 = 1/(4 * ^1J_{CH})$ and $Δ_{1'} = 1/(8 * ^1J_{CH})$ and δ stand for the duration of a pulsed field gradient and its recovery delay. A λ-scaled evolution period is incorporated for the selective monitoring of terms I and II which are detected in separate FID1 and FID2 periods, respectively. The spectral width in the indirect dimension (SW1) is set to $1/(2 * λ * Δt_1)$ and $1/(2 * Δt_1)$ for FID1 and FID2 datasets, respectively. A minimum phase cycle is used: $ϕ_1 = x, −x$ and $ϕ_r = x, −x$. More details can be found in the experimental section.

applied to remove any residual magnetization coming from term I and a last 90° (^{1}H) pulse flips term II to the transverse plane, which is detected during the FID2 period. For a proper selection of both CTPs, gradients G2, G3 and G5 are set to 40%, 20.1% and 10.05% according to Eqs. (2) and (3):

$$\text{Term I(FID1)}: \ p1 * G2 * \gamma_C + p1 * G2 * \gamma_C - G3 * \gamma_H = 0 \tag{2}$$

$$\text{Term 2(FID2)}: \ p1 * G2 * \gamma_C - G5 * \gamma_H = 0 \tag{3}$$

Data acquisition in FID1 and FID2 are made in identical conditions, and therefore the detected F2 dimension in both spectra is the same. The SADA-HSQC experiment yields a 2D HSQC spectrum with its full spectral width (SW1^{normal}) in FID 2 whereas an aliased HSQC spectrum showing a reduced SW1^{aliased} according to the λ factor is obtained in FID1:

$$\text{SW1}^{aliased} = \text{SW1}^{normal}/\lambda \tag{4}$$

The practical aspects of the new SADA-HSQC technique are here assessed regarding the importance of the inter-pulse delay optimization, the relationship between the λ scaling factor and the digital resolution in F1, the duration of FID periods and their effects on sensitivity in both FID1 and FID2 data. Also, the influence of the number of increments to be collected and the overall experimental times that can recommend the use of the MFA approach instead of the conventional sequential step-by-step acquisition is discussed. The performance of the SADA-HSQC experiment has been verified using a test sample of the cyclic peptide cyclosporine dissolved in CDCl$_3$ that was also used to evaluate the performance of previous spectral aliased HSQC methods [13–15,19]. The collection of a set of different experiments varying the λ factor, the number of increments and the duration of the FIDs was performed. Initially, the acquisition conditions included 128 increments and SW1 = 100 ppm. Fig. 2 shows the 2D HSQC spectra obtained from FID1 and FID2 in the SADA-HSQC scheme after conventional Four-
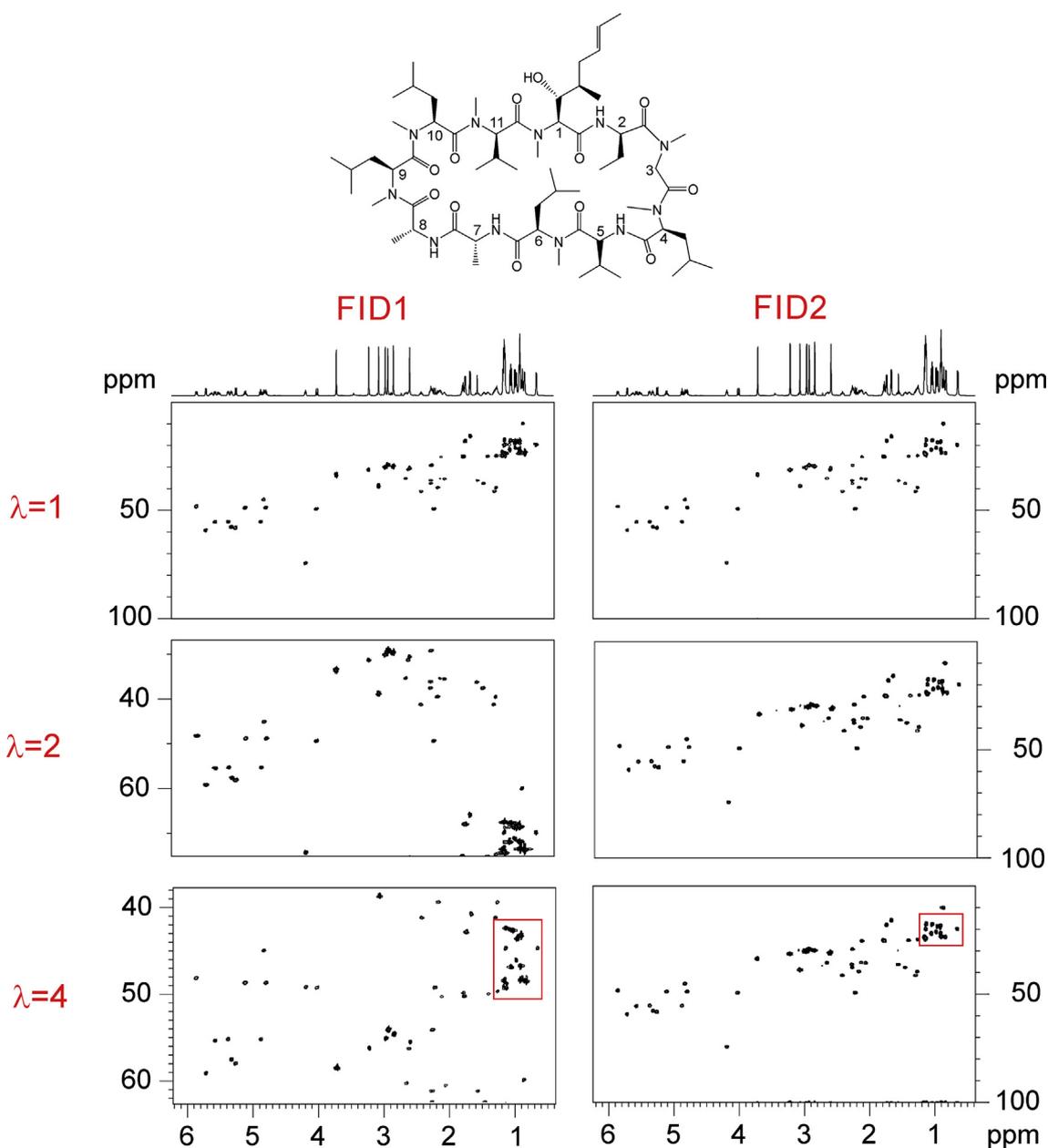

Fig. 2. (Left) Spectral-aliased (FID1) and (Right) conventional (FID2) 2D HSQC spectra of the peptide cyclosporine in CDCl$_3$ acquired simultaneously with the SADA-HSQC pulse scheme, with λ-scaling factors of 1, 2 and 4. SW1 in FID1 are 100, 50 and 25 ppm, respectively. Note that the aliphatic methyl signals are better dispersed in the FID1 spectrum, as shown in the highlighted boxes.

ier transformation, using λ factors of 1, 2 and 4. As shown, FID2 always affords the regular HSQC spectrum with its full SW1^{normal} (100 ppm) whereas FID1 yields the corresponding aliased HSQC spectrum according to the applied λ factor, with SW1^{aliased} of 100, 50 and 25 ppm, respectively. At first glance, the complementarity and different DR1 between the two spectra is displayed in the region of the aliphatic methyl signals highlighted in boxes.

Fig. 3 compares the relative sensitivities achieved for each FID1 and FID2 datasets in experiments recorded with scaling factors of λ = 1, 8 and 16. In the basic experiment acquired with λ = 1, FID2 affords the same spectrum (same SW1) than FID1 but differing of the signal intensities due to different factors. Most of the signal attenuation observed in FID1 is due to the additional gradient CTP selection applied in the second t_1 period. In addition, signal

intensity for the different CH_n multiplicities strongly depends on $\Delta_{1'}$ and Δ_1 delays optimization (see Fig. S3 for simulations). When λ is increased, the overall sensitivity in both FID1 and FID2 is attenuated by ∼10% and ∼20% for λ = 8 and λ = 16, respectively, due to T_2 relaxation effects as similarly observed when comparing conventional HSQC and SA-HSQC spectra. In these cases, t_1^{max} is 8.48, 67.85 and 135.7 ms for λ = 1, 8 and 16, respectively. The practical limits on important parameters such as the optimum λ factors, the SW1 to be monitored and the FID1/FID2 durations depend on each sample, as a function of the existing signal overlapping and the T_2 relaxation times. Despite the mentioned sensitivity drawbacks, SADA-HSQC experiments with high λ factors corresponding to SW1 of 1–2 ppm can be executed for a medium-sized molecule like cyclosporine (MW = 1202) with an obvious progressive signal
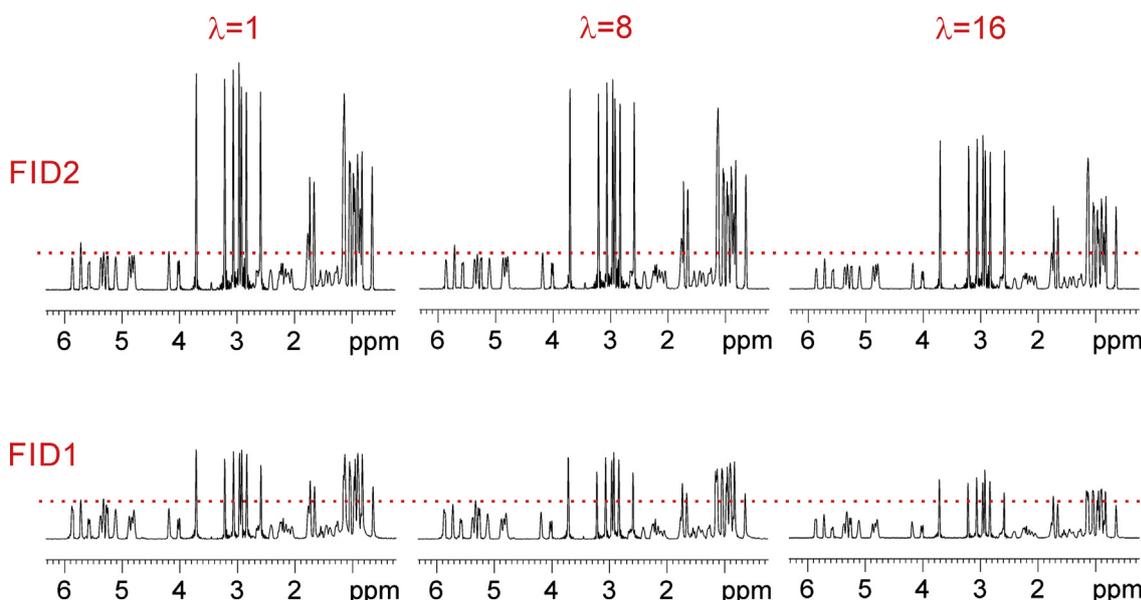

Fig. 3. 1D internal F2 projections to correlate relative sensitivities for the (bottom) SA-HSQC (FID1) and (top) HSQC (FID2) spectra simultaneous collected with the SADA-HSQC pulse scheme, with λ scaling factors of 1, 8 and 16.
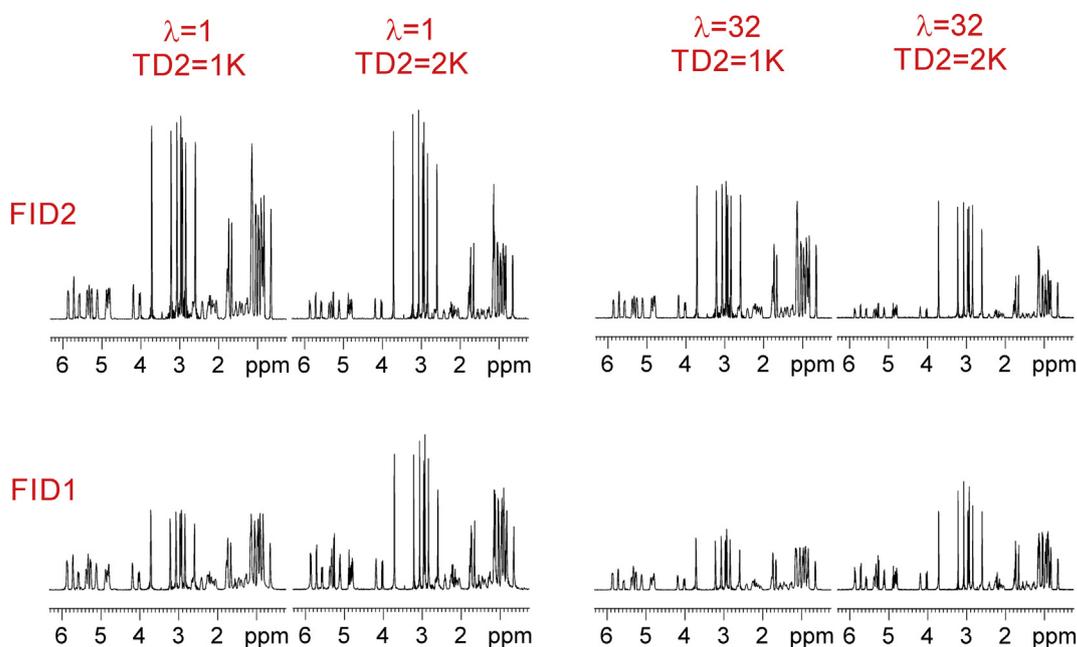

Fig. 4. 1D internal projections extracted from the F2 dimensions in (bottom) spectral-aliased (FID1) and (top) conventional (FID2) 2D HSQC spectra obtained simultaneously from the SADA-HSQC pulse scheme using λ values of 1 and 32, and TD2 of 1 K and 2 K.

decrease but with very high levels of DR1 that can reach 2–4 Hz/pt before data transformation, of the same order as what is obtained in conventional 1D ^{13}C spectra. Experimental times of HSQC, SA-HSQC, SADA-HSQC (with different λ factors) experiments are shown in Tables S1–S2. The implementation of SA in conventional HSQC experiments only lengthens the duration of the SA-HSQC experiment by 5% due to t_1^{max}. Regarding spectrometer times, SADA-HSQC is collected in about the 55% of the time needed for the separate acquisition of HSQC and SA-HSQC experiments.

Another key parameter to evaluate the feasibility of MFA experiments is the duration of the FID1 and FID2 periods (AQ) which defines the resolution in the acquisition dimension. Using routine conditions such as TD2 of 1024 points and SW2 = 10 ppm, the duration of each FID is 85 ms. Doubling TD2 to 2048 points, AQ is extended to 170 ms. Fig. 4 compares the experimental sensitivities achieved when $\lambda = 1$ and $\lambda = 32$ and using TD2 values of 1 K and 2 K. As it can be observed, the extension of AQ is beneficial for FID1 because the better resolution offers sharper lines and therefore improved sensitivity ($\sim$20%), more than compensating for the relaxation effects due to the increased t_1^{max}. Otherwise, the sensitivity of FID2 is decreased by $\sim$25% due to the potential losses by diffusion and/or relaxation effects. However, this loss is irrelevant because the sensitivity in FID1 is the limiting factor in the SADA-HSQC experiment. As a conclusion, the duration of AQ

and therefore the resolution in F2 is not a limitation in the performance of SADA-HSQC experiments.

When sensitivity is not the limiting factor, SADA-HSQC experiments can be recorded with only two scans per increment. To maximize spectrometer time efficiency and to achieve maximum F1 resolution per time unit, the acquisition of the SADA-HSQC experiment using a low number of increments may be advisable. Fig. 5 shows the results obtained for a different number of increments (from 16 to 128). For instance, collecting only 64 increments with SW1 = 100 ppm, the increment Δt_1 value is set to 66.26 µs and a DR1 of 235.8 Hz/pt. On the other hand, the aliased spectrum (with $\lambda = 32$) acquired simultaneously yields an SW1 = 5 ppm and Δt_1 of 2.12 ms, affording an increase of resolution by a factor of 32 up to 7.37 Hz/pt. Under these conditions, the DR1 provided by the SA spectrum would equal to a conventional spectrum recorded with 2048 increments. The SADA-HSQC experiment acquired with $\lambda = 32$ and TD1 = 64 is quickly executed in about 3 min. It is shown how the lack of resolution of FID2 is compensated with the superb resolution and signal dispersion achieved in FID1, even collecting only 16 increments, allowing clear signal identification and assignment as well as of the accurate determination of chemical shift values in very reduced spectrometer times.

Fig. 6 shows the expansion of the aliphatic methyl region of both HSQC and SA-HSQC spectra acquired simultaneously with the SADA-HSQC experiment using $\lambda = 32$ and 64 increments. SW1
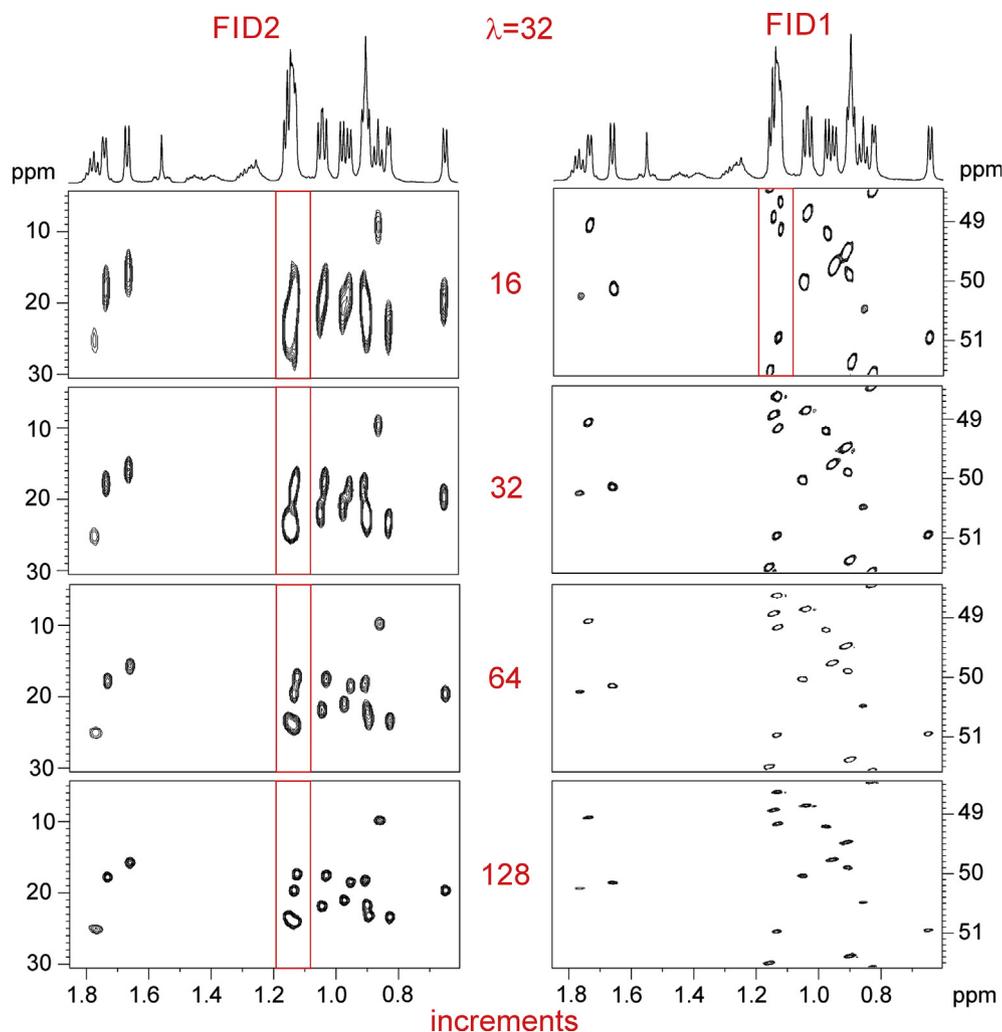

Fig. 5. Expansions of the aliphatic methyl region corresponding to the HSQC (SW1 = 100 ppm) and SA-HSQC (SW1 = 3.125 ppm) spectra acquired simultaneously with the SADA-HSQC experiment with $\lambda = 32$ and TD1 values from (top) 128 to (bottom) 16 increments. The ^{13}C offset of the original experiment was set to 50 ppm.
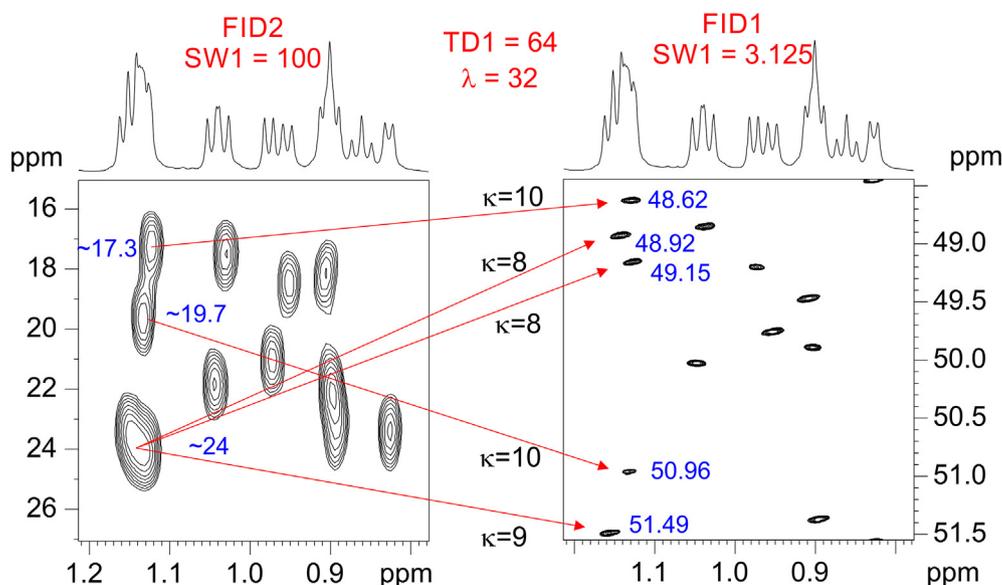
Fig. 6. Expansions of the HSQC (SW1 = 100 ppm) and SA-HSQC (SW1^{aliased} = 3.125 ppm) spectra acquired simultaneously with the SADA-HSQC experiment with $\lambda = 32$ and TD1 = 64 increments. The ^{13}C offset of the original experiment was set to 50 ppm. The experimental time to record both datasets was 3 min. All methyl signals in FID1 are distinguished, and their chemical shifts accurately determined using the relationship $\delta(^{13}C)^{aliased} = \delta(^{13}C)^{true} \pm \kappa * 3.125$.

are set to 100 ppm and 3.125 ppm for FID2 and FID1, respectively. Note how the non-resolved cross-peaks in the regular low-resolved HSQC spectrum are dispersed in the highly-resolved SA spectrum. The reference spectrum is needed to obtain a rough estimation of δ (^{13}C)^{true}, and it is fundamental to deduce the κ factor observed for each cross-peak in the aliased spectrum. All methyl signals in FID1 can be distinguished, and their chemical shifts accurately determined to apply meticulously the relationship described in Eq. (1). For instance, note the excellent dispersion achieved for the fully overlapped five Me signals resonating in the narrow ^{1}H range between 1.13 and 1.17 ppm.

3. Conclusions

In summary, we have proposed an interesting NMR strategy to obtain high levels of digital resolution and spectral dispersion per time unit in the HSQC experiment. It has been shown that conventional and aliased 2D HSQC spectra can be simultaneous collected using a single pulse sequence, in minutes and a full automation mode. The method does not require many t_1 increments because accurate chemical shift determinations can be performed from the highly-resolved aliased spectrum. The signal-dependent κ aliasing factors are determined by comparing chemical shift values from the regular and the aliased HSQC spectra. The method described here is also suitable to record two aliased 2D HSQC spectra by scaling the two different t_1 periods differently [10,14,19], it is extensible to other HSQC-like experiments and also compatible with computer-assisted spectral reconstruction methods developed to obtain high-resolution NMR spectra with their full spectral width representation.

4. Experimental part

NMR spectra were recorded on a Bruker AVANCE spectrometer equipped with a 5 mm TBI probehead operating at 600.13 MHz for ^{1}H at 298 K. The sample used in this work was 25 mM of cyclosporine dissolved in 0.6 ml of C_6D_6. The pre-scan delay was set to 1 s, and two scans for each one of the 128 t_1 increments were acquired (1024 points of time domain in the acquisition dimension). Spectral widths in the detected (SW2) and indirect (SW1) dimensions

were 10 ppm (6009 Hz) and 100 ppm (15,091 Hz), respectively. The acquisition time (AQ) for each FID1 and FID2 period was of 85 ms. The inter-pulse delays were optimized to 140 Hz ($\Delta_1 = 1.78$ ms and $\Delta_{1'} = 0.89$ ms) and the gradient ratio G1:G2: G3:G4:G5 was set to 11:40:20.1:$-$17:10.05 (gradient shape SINE.100). The overall duration involving the gradient (1 ms) and its recovery delay was 1.02 ms (δ). A basic two-step phase cycling was applied: $\Phi_1 = x, -x$; $\Phi_{rec.} = x, -x$. Comparison of experimental times and FID resolution before processing along the F1 dimension between the standard HSQC, spectral aliased HSQC and several λ-scaled SADA-HSQC experiments are summarized in Tables S1–S2.

SADA-HSQC experiments were acquired using the echo/anti-echo protocol where the gradient G2 was inverted for every second FID. All data is individually processed in the usual way using a zero-filling in both F1 and F2 dimensions, up 2048 and 1024 data matrix respectively, and applying a non-shifted sine-bell window function in both dimensions before Fourier transformation. For processing, the automation AU program splitx rewrites the original FID1 and FID2 data allocated in different memory blocks to independent files. FID1 is transformed with the AU program fix_ali to recalculate SW1, according to the λ scaling factor. The SADA-HSQC pulse program is available in the SI.

Appendix A. Supplementary material

Supplementary data associated with this article can be found, in the online version, at https://doi.org/10.1016/j.jmr.2019.01.004.

References

[1] C. Dalvit, Semi-selective two-dimensional homonuclear and heteronuclear NMR experiments recorded with pulsed field gradients, Magn. Reson. Chem. 33 (1995) 570–576, https://doi.org/10.1002/mrc.1260330713.

[2] C. Gaillet, C. Lequart, P. Debeire, J.M. Nuzillard, Band-selective HSQC and HMBC experiments using excitation sculpting and PFGSE, J. Magn. Reson. 139 (1999) 454–459, https://doi.org/10.1006/jmre.1999.1808.

[3] J.C. Hoch, M.W. Maciejewski, M. Mobli, A.D. Schuyler, A.S. Stern, Nonuniform sampling and maximum entropy reconstruction in multidimensional NMR, Acc. Chem. Res. 47 (2014) 708–717, https://doi.org/10.1021/ar400244v.

[4] K. Kazimierczuk, J. Stanek, A. Zawadzka-Kazimierczuk, W. Koźmiński, Random sampling in multidimensional NMR spectroscopy, Prog. Nucl. Magn. Reson. Spectrosc. 57 (2010) 420–434, https://doi.org/10.1016/j.pnmrs.2010.07.002.

[5] M. Mobli, J.C. Hoch, Nonuniform sampling and non-Fourier signal processing methods in multidimensional NMR, Prog. Nucl. Magn. Reson. Spectrosc. 83 (2014) 21–41, https://doi.org/10.1016/j.pnmrs.2014.09.002.

[6] W.F. Reynolds, R.G. Enriquez, The advantages of forward linear prediction over multiple aliasing for obtaining high-resolution HSQC spectra in systems with extreme spectral crowding, Magn. Reson. Chem. 41 (2003) 927–932, https://doi.org/10.1002/mrc.1271.

[7] L.E. Kay, P. Keifer, T. Saarinen, Pure absorption gradient enhanced heteronuclear single quantum correlation spectroscopy with improved sensitivity, J. Am. Chem. Soc. 26 (1992) 10663–10665, https://doi.org/10.1021/ja00052a088.

[8] J. Schleucher, M. Schwendinger, M. Sattler, P. Schmidt, O. Schedletzky, S.J. Glaser, O.W. Sørensen, C. Griesinger, A general enhancement scheme in heteronuclear multidimensional NMR employing pulsed field gradients, J. Biomol. NMR 4 (1994) 301–306, https://doi.org/10.1007/BF00175254.

[9] D. Jeannerat, Rapid multidimensional NMR: high resolution by spectral aliasing, Encycl. Magn. Reson. (2011), https://doi.org/10.1002/9780470034590.emrstm1187.

[10] I. Baskyr, T. Brand, M. Findeisen, S. Berger, Acquisition regime for high-resolution heteronuclear 2D NMR spectra, Angew. Chem. Int. Ed. 45 (2006) 7821–7824, https://doi.org/10.1002/anie.200603036.

[11] A. Cotte, M. Foroozandeh, D. Jeannerat, Combination of homonuclear decoupling and spectral aliasing to increase the resolution in the 1H dimension of 2D NMR experiments, Chim. Int. J. Chem. 66 (2012) 764–769, https://doi.org/10.2533/chimia.2012.764.

[12] A. Cotte, D. Jeannerat, 1D NMR homodecoupled (1)H spectra with scalar coupling constants from 2D NemoZS-DIAG experiments, Angew. Chem. Int. Ed. 54 (2015) 6016–6018, https://doi.org/10.1002/anie.201500831.

[13] D. Jeannerat, Computer optimized spectral aliasing in the indirect dimension of 1H–13C heteronuclear 2D NMR experiments. A new algorithm and examples of applications to small molecules, J. Magn. Reson. 186 (2007) 112–122, https://doi.org/10.1016/j.jmr.2007.02.003.

[14] M. Foroozandeh, D. Jeannerat, Reconstruction of full high-resolution HSQC using signal split in aliased spectra, Magn. Reson. Chem. 53 (2015) 894–900, https://doi.org/10.1002/mrc.4283.

[15] K. Ramírez-Gualito, D. Jeannerat, Exploiting the phase of NMR signals to carry useful information. Application to the measurement of chemical shifts in aliased 2D spectra, Magn. Reson. Chem. 53 (2015) 901–907, https://doi.org/10.1002/mrc.4301.

[16] G.B.B. Njock, T.A. Bartholomeusz, M. Foroozandeh, D.E. Pegnyemb, P. Christen, D. Jeannerat, NASCA-HMBC, a new NMR methodology for the resolution of severely overlapping signals: application to the study of agathisflavone, Phytochem. Anal. 23 (2012) 126–130, https://doi.org/10.1002/pca.1333.

[17] B. Vitorge, S. Bieri, M. Humam, P. Christen, K. Hostettmann, O. Muñoz, S. Loss, D. Jeannerat, High-precision heteronuclear 2D NMR experiments using 10-ppm spectral window to resolve carbon overlap, Chem. Commun. (2009) 950–952, https://doi.org/10.1039/b820478k.

[18] D. Jeannerat, High resolution in heteronuclear 1H–13C NMR experiments by optimizing spectral aliasing with one-dimensional carbon data, Magn. Reson. Chem. 41 (2003) 3–17, https://doi.org/10.1002/mrc.1118.

[19] M. Foroozandeh, D. Jeannerat, Deciphered chemical shifts in aliased spectra recorded with two slightly different narrow windows or differential chemical shift evolution, ChemPhysChem 11 (2010) 2503–2505, https://doi.org/10.1002/cphc.201000421.

[20] M. Pérez-Trujillo, L. Castañar, E. Monteagudo, L. Kuhn, P. Nolis, A. Virgili, R.T. Williamson, T. Parella, Simultaneous 1H and 13C NMR enantiodifferentiation from highly-resolved pure shift HSQC spectra, Chem. Commun. 50 (2014) 10214–10217, https://doi.org/10.1039/C4CC04077E.

[21] L. Castañar, R. Roldán, P. Clapés, A. Virgili, T. Parella, Disentangling complex mixtures of compounds with near-identical 1H and 13C NMR spectra using pure shift NMR spectroscopy, Chem. - A Eur. J. 21 (2015) 7682–7685, https://doi.org/10.1002/chem.201500521.

[22] N. Marcó, A. Fredi, T. Parella, Ultra high-resolution HSQC: Application to the efficient and accurate measurement of heteronuclear coupling constants, Chem. Commun. 51 (2015) 3262–3265, https://doi.org/10.1039/c4cc10279g.

[23] K. Motiram Corral, M. Pérez-Trujillo, P. Nolis, T. Parella, Implementing one-shot multiple-FID acquisition into homonuclear and heteronuclear NMR experiments, Chem. Commun. 54 (2018) 13507–13510, https://doi.org/10.1039/C8CC08065H.

[24] P. Nolis, M. Pérez-Trujillo, T. Parella, Multiple FID acquisition of complementary HMBC data, Angew. Chem. Int. Ed. 46 (2007) 7495–7497, https://doi.org/10.1002/anie.200702258.

[25] P. Nolis, K. Motiram-Corral, M. Pérez-Trujillo, T. Parella, Interleaved Dual NMR acquisition of equivalent transfer pathways in TOCSY and HSQC experiments, ChemPhysChem (2018), https://doi.org/10.1002/cphc.201801034.